Structural distortions and magnetisms in Fe-doped $LaMn_{1-x}Fe_xO_3$ ($0 < x \leq 0.6$)*

Zheng Long(郑 龙) and Wu Xiao-Shan(吴小山)†

Laboratory of Solid State Microstructures and Department of Physics, Nanjing University, Nanjing 210093, *China*

(Received 21 March 2013; revised manuscript received 19 April 2013)

X-ray absorption spectra (XAS) at Mn K-edge and Fe K-edge in $LaMn_{1-x}Fe_xO_3$ show that with the increase of Fe substitution the chemical valence of Mn^{4+} decreases, while the chemical valence of Fe^{3+} remains unchanged. Structural distortions, such as the rotating and tilting for oxygen octahedron in the unit cell vary with iron content. A phase transition occurs at the Fe content values of 0.2∼0.3. The evolutions of rotation and tilting angle of FeO_6/MnO_6 octahedral may be the vital factors to the structure and magnetism. We believe that the spin configuration of Fe^{3+} may vary from the intermediate spin $t_{2g}^4e_g^1$ ($S = 3/2$) to the higher spin $t_{2g}^3e_g^2$ ($S = 5/2$) near the phase transition.

Keywords: structural distortion, X-ray absorption, phase transition

PACS: 78.70.Dm, 36.40.Cg, 61.05.cp **DOI:** 10.1088/1674-1056/22/10/107806

1. Introduction

Perovskite family oxides ABO_3 are particularly interesting materials, as their ground states are derived from the competition among lattice, spin, charge, and orbital degrees of freedom.[1,2] Octahedron BO_6 is the origin of many diverse properties in perovskite.[3,4] With slight substitution of elements at A or B site, the octahedron may distort with tilting and rotating and produces much more fascinating properties.[5–8] The origins of those diverse properties and the inner structure distortion have attracted much attention.

Much research done so far has focused on the properties of $LaMnO_3$, by producing lattice distortions using chemical substitution.[9] The ionic radius of Fe^{3+} (0.645 Å, 1 Å = 0.1 nm) is nearly equal to that of Mn^{3+} (0.645 Å), but larger than that of Mn^{+4} (0.53 Å),[10] so Fe^{3+} is believed to replace Mn^{3+} in manganite easily but to substitute for Mn^{4+} in manganite difficultly.[11] On the other hand, the excess oxygen is believed to play an important role for unit cell symmetry, which may change from rhombohedral to orthorhombic, the magnetism may also vary with the oxygen content.[12,13]

The magnetic properties in iron-doped $LaMn_{1-x}Fe_xO_3$ have been studied.[14] However, the spin configuration for Fe and Mn, the correlation between magnetic interaction and structure evolution in the compound are still elusive,[15] which may be very important for understanding physics in manganite. In the present paper, single phase $LaMn_{1-x}Fe_xO_3$ with $x = 0$–0.6 are synthesized. Their detailed structures and spin configurations are studied.

2. Experiment

Single phase $LaMn_{1-x}Fe_xO_3$ ($x = 0$–0.6) polycrystals are prepared by traditional solid-state reaction technique in air. Stoichiometric mixtures of high pure powders of La_2O_3, Fe_2O_3, and MnO_2, are ground and calcined in air for 24 h at 1250 °C. The details of the sample preparation are described elsewhere.[16,17] The crystal structure is studied by X-ray diffraction (XRD) carried out at the beam line BL14B located at Shanghai Synchrotron Radiation Facility (SSRF). XRD data are collected in a step scaning mode in steps of 0.02° in 2θ. The temperature dependences of magnetization M–T under both zero field cooling (ZFC) and field cooling (FC) condition are measured by using a Quantum Design superconducting quantum interference device (SQUID), with a magnetic field of 100 Oe (1 Oe = 79.5775 A·m^{-1}) applied. X-ray absorption data at Mn K-edge and Fe K-edge for all samples are collected at room temperature in transmission mode at beam line BL14W1 on SSRF.

3. Results and discussion

The little lattice is expected to be distorted after Fe^{3+} has substituted for Mn^{3+}. Such a substitution of Fe^{3+} for Mn^{3+} is realizable due to the ion radii of Fe^{3+} and Mn^{3+} ions being similar. XRD studies reveal that our samples ($LaMn_{1-x}Fe_xO_3$ ($x = 0$–0.6)) are all of single phase, but with a phase transition from rhombohedral symmetry $R\bar{3}c$ to orthorhombic symmetry $Pbnm$ at $0.2 \leq x \leq 0.3$. We perform detailed structure analyses for $LaMn_{1-x}Fe_xO_3$ through the Rietveld refinements[18] as done in our previous papers.[19,20] Table 1 lists unit cell parameters for samples with $x = 0$, 0.05, 0.1, 0.15, 0.2, 0.3, 0.4,

*Project supported by the State Key Program for Basic Research of China (Grant No. 2010CB923404) and the National Natural Science Foundation of China (Grant Nos. 11274153, 11204124, and 51202108).

†Corresponding author. E-mail: xswu@nju.edu.cn

© 2013 Chinese Physical Society and IOP Publishing Ltd

0.5, and 0.6. Typical XRD patterns with the refinements and the difference for samples with $x = 0.1$ and $x = 0.4$ are shown in Fig. 1.

Table 1. Unit cell parameters of room-temperature $LaMn_{1-x}Fe_xO_3$ ($x = 0$–0.6).

x	Space group	a/Å	b/Å	c/Å	Volume/Å^3
0	$R\bar{3}c$	5.5279		13.3448	353.164
0.05	$R\bar{3}c$	5.5274		13.3537	353.327
0.1	$R\bar{3}c$	5.5301		13.3613	353.867
0.15	$R\bar{3}c$	5.5310		13.3676	354.152
0.2	$R\bar{3}c$	5.5238		13.4070	354.278
0.3	*Pbnm*	5.5398	5.5141	7.8083	238.519
0.4	*Pbnm*	5.5343	5.5215	7.8170	238.874
0.5	*Pbnm*	5.5377	5.5267	7.8268	239.542
0.6	*Pbnm*	5.5398	5.5314	7.8332	240.035

All refinements fit well to experimental results. The unit cell volume increases with Fe content increasing as shown in Fig. 2(b). Due to the Mn–O–Mn ferromagnetic (FM) super-exchange coupling in the *ab* plane and anti-ferromagnetic (AFM) double-exchange (DE) coupling in the *c* direction in $LaMnO_3$,[21] we can anticipate a change of magnetic interaction effect to the structure evolution during Fe substitution.

To make the magnetic interaction in $LaMn_{1-x}Fe_xO_3$ clear, the structural distortions of $FeO_6/MnO_6(BO_6)$ octahedrons are investigated.[22] The rotation angle is defined as the difference between 180° and B–O_{ab}–B angle, while the tilting angle is defined as the difference between 180° and B–O_c–B angle along *c* axis as shown in Fig. 2(a). Refinements show that the variations of these structural parameters coincide with the evolutions of rotation and tilting of the FeO_6/MnO_6 octahedral. When $x < 0.2$, both the rotation angle and tilting angle increase slightly with x increasing as shown in Fig. 2(b).

At $0.2 \leq x \leq 0.3$, there is a phase transition from $R\bar{3}c$ to *Pbnm*, the tilting angle becomes very stable while the rotation angle increases rapidly. The results indicate that with the gradual increase of Fe substitution, the rotation effect between the two octahedrals is gradually enhanced in the *ab* plane while the tilting effect is not enhanced further in the *c* direction. The rotation angle and tilting angle are nearly equal to 11° at $x = 0.6$, and the two angles may increase very slightly with Fe doping increasing when $x > 0.6$ in $LaMn_{1-x}Fe_xO_3$.[23]

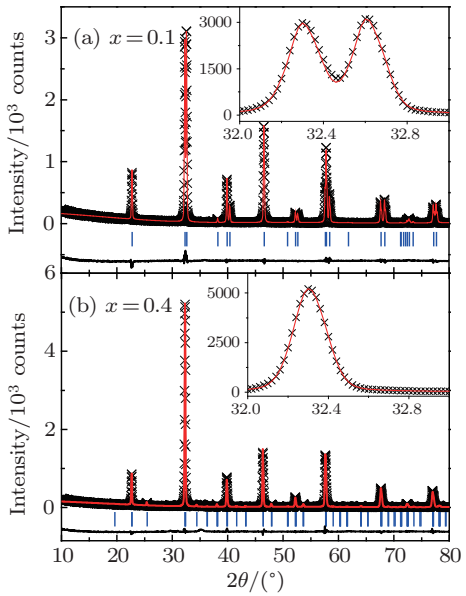


Fig. 1. (color online) X-ray diffraction data (×), refinements (line) for the samples (a) $LaMn_{0.9}Fe_{0.1}O_3$ with space group $R\bar{3}c$, and (b) $LaMn_{0.6}Fe_{0.4}O_3$ with space group *Pbnm*. Marks with short bar (|) indicate positions of Bragg reflections, the difference between observed and calculated curve at the bottom. Inserts show the reflections near 32°, indicating phase transition.

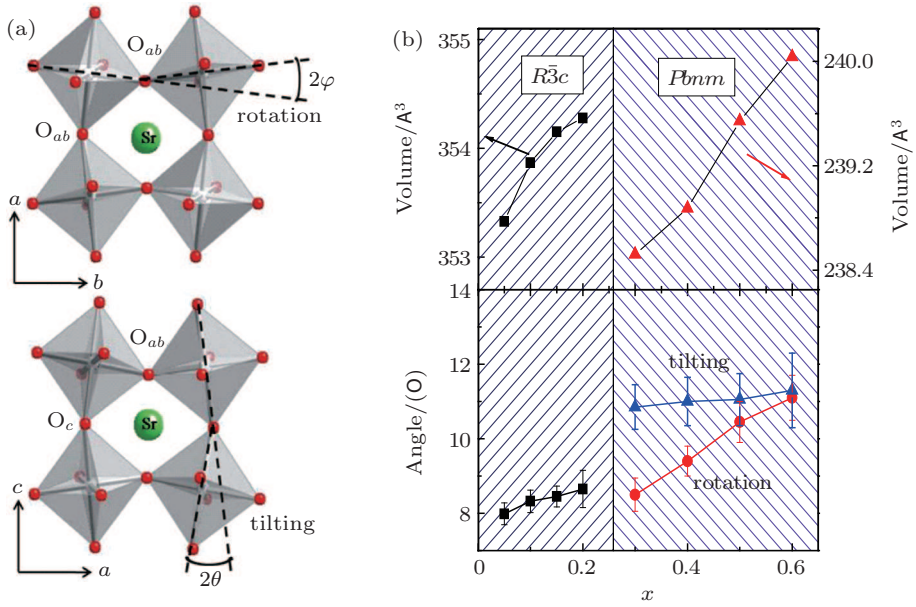


Fig. 2. (color online) (a) Schematic illustration of MnO_6/FeO_6 octahedral rotation and tilting effect in $LaMn_{1-x}Fe_xO_3$. (b) (upper) Unit cell volume evolution with the increase of Fe content x in $LaMn_{1-x}Fe_xO_3$. (down) Rotating and tilting angles each as a function of Fe content x. The symmetry area is identified as seen in the figure.

If the excess oxygen effect on this system plays some roles in this structural phase transition, the chemical valence of Mn^{4+} due to excess oxygen may gradually change into that of Mn^{3+} with the increase of Fe substitution. X-ray absorption fine structure (XAFS) experiment at the Mn K-edge of the sample at room temperature is carried out to investigate the chemical valence. Figure 3 shows the normalized XAFS spectra of the Mn K edge and Fe K-edge for $LaMn_{1-x}Fe_xO_3$ ($x = 0.1$–0.4).

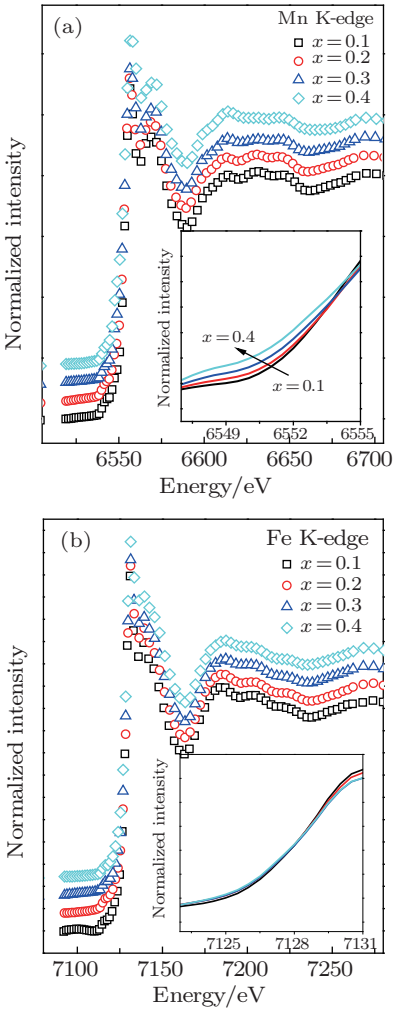


Fig. 3. (color online) Normalized XAFS spectra of $LaMn_{1-x}Fe_xO_3$ ($x = 0.1$–0.4) at (a) Mn K edge and (b) Fe K-edge. Insets show the near absorption edges of the spectra.

The absorption edge of Mn in the X-ray absorption near edge structure (XANES) spectrum is expected to shift when the valence state of manganese is changed. There is a clear shift toward lower energy of Mn absorption edge with the increase of Fe content (Fig. 3(a)), while the absorption edge of Fe remains nearly unchanged with Fe substitution variation (Fig. 3(b)). This is the clear evidence of the existence of Mn^{4+} in this system and the Mn^{4+} gradually changes into Mn^{3+} with Fe content increasing. While the Fe ions exhibit Fe^{3+} ions, they are not affected by the excess oxygen.

Mn^{3+}, Mn^{4+}, and Fe^{3+} are strongly coupled in this system. Figure 4 shows the temperature dependences of magnetization under zero-field cooling (ZFC) and field-cooling (FC) for all samples. As Fe doping is accompanied with the decrease of the Mn^{4+}, the number of DE interactions of Mn^{3+}–O–Mn^{4+} gradually decreases. As a result, the paramagnetic (PM)–ferromagnetic (FM) transition temperature gradually decreases as can be seen in Fig. 4.

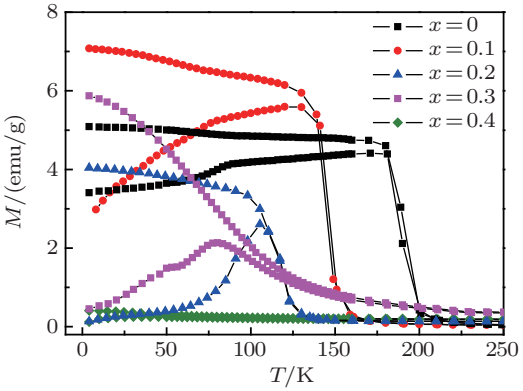


Fig. 4. (color online) Temperature dependences of magnetization under zero-field cooling (ZFC) and field cooling (FC) for $LaMn_{1-x}Fe_xO_3$ with $x = 0$–0.4.

In addition, Mn ions and Fe ions are believed to be ferromagnetically coupled at low temperature.[24] The ZFC and FC behavior mean that the cluster-spin glass states are formed[25] as the transition width becomes wider with Fe content increasing. Although with the gradual increase of Fe substitution, the ferromagnetism in $LaMn_{1-x}Fe_xO_3$ is suppressed, it can be seen that the magnetization of the sample with $x = 0.3$ is higher than that of the sample with $x = 0.2$, which is in consistence with that reported by Tong *et al.*[26]

Here we discuss the structural evolution and the magnetic property in $LaMn_{1-x}Fe_xO_3$. When $x < 0.2$, both the rotation and tilting effect are enhanced. Fe ion in $LaMn_{1-x}Fe_xO_3$ is magnetically coupled with Mn ion due to DE interaction at low temperature.[10,26] Although Fe ions are ferromagnetically coupled with Mn ions at low temperature, the gradually reducing magnetization indicates that DE interaction of Mn^{3+}–O–Mn^{4+} is very strong in $LaMn_{1-x}Fe_xO_3$.

When $x > 0.3$, due to the phase transition, the rotation angle and tilting angle become quite different from each other, and with the increase of Fe content the two angles are nearly equal to each other. The similarity in the rotation angle and tilting angle may indicate the exchange effect between FeO_6 and MnO_6 octahedrons in $LaMn_{1-x}Fe_xO_3$ when $x \geq 0.6$[23] as there exist both super-exchange (SE) effect and DE effect in $LaMnO_3$.[21]

As the absorption edge of Mn gradually shifts toward lower energy, we may draw the conclusion that the excess oxygen does affect the structure transition. With the decrease of

oxygen content in the unit cell, the exchange effect through O ions may change. Due to the DE effect and SE effect between Mn and Fe, the spin state of Fe should be taken into consideration, with Fe substitution increased.

Tong *et al.*[26] and Zhou *et al.*[12] proved that the Fe^{3+} ion in $LaMn_{1-x}Fe_xO_3$ is in the $t_{2g}^4e_g^1$ state when the system is at $R\bar{3}c$ symmetry. On the other hand, $LaFeO_3$ is known as a G-type anti-ferromagnetic insulator, in which Fe^{3+} ion is in the high-spin state, i.e., with the localized electron configuration of Fe^{3+} ($t_{2g}^3e_g^2$).[27,28] In our present case, an Fe^{3+} spin state transition between the intermediate spin state ($t_{2g}^4e_g^1$) and the high spin state ($t_{2g}^3e_g^2$) happens with the Fe content in $LaMnO_3$ increasing gradually.

The magnetization for a sample with $x = 0.3$ is higher than that for a sample with $x = 0.2$ in Fig. 4, which may be explained as the spin state transition, i.e., the phase transition accompanied with a spin state transition of Fe^{3+} from the intermediate spin ($S = 3/2$) state to the high spin ($S = 5/2$), as a result, the FM moment between Mn^{3+}–O–Fe^{3+} is enhanced.

4. Conclusions

Polycrystalline single phase $LaMn_{1-x}Fe_xO_3$ ($x = 0$–0.6) is synthesized by using the traditional solid-state reaction method. The PM–FM transition temperature gradually decreases with Fe content increasing. In addition, the ZFC and FC measurements at low temperature indicate the cluster-spin glass states. XAFS results indicate that with Fe content increasing, Mn^{4+} ion gradually changes into Mn^{3+} ion, while Fe^{3+} ion remains unchanged. The Fe^{3+} spin state may vary from an intermediate spin state to a high spin state. The evolutions of rotation and titling angle, when structural phase transition occurs, may also reveal the spin state transition, and the rotation angle and tilting angle, which are nearly the same, may indicate the exchange effect between octahedrons in $LaMn_{1-x}Fe_xO_3$ when $x \geq 0.6$.

Acknowledgments

This work was done using the BL14W1 and BL14B beam lines (Shanghai Synchrotron Radiation Facility).

References

[1] Ahn K H, Wu X W, Liu K and Chien C L 1996 *Phys. Rev. B* **54** 15299
[2] Jin J L, Zhang X Q, Li G K, and Cheng Z H 2012 *Chin. Phys. B* **21** 107501
[3] De K, Ray R, Panda R N, Giri S, Nakamura H and Kohara T 2005 *J. Magn. Magn. Mater.* **288** 339
[4] De K, Patra M, Majumdar S and Giri S 2007 *J. Phys. D: Appl. Phys.* **40** 7614
[5] Gu M Q, Xie Q, Shen X, Xie R B, Wang J L, Tang G, Wu D, Zhang G P and Wu X S 2012 *Phys. Rev. Lett.* **109** 157003
[6] Gu M Q, Wang J L, Wu X S and Zhang G P 2012 *J. Phys. Chem. C* **116** 24993
[7] Zheng L, Lu Yi, Zhao J J, Zhang X Q, Xing R, Wu H Y, Jin X, Zhou M and Cheng Z H 2010 *Chin. Phys. B* **19** 127501
[8] Peng J, Qu Z, Qian B, Fobes D, Liu T J, Wu X S, Pham H M, Spinu L M S and Mao Z Q 2010 *Phys. Rev. B* **82** 024417
[9] Patra M, De K, Majumdar S and Giri S 2007 *Eur. Phys. J. B* **58** 367
[10] Zhou X D, Yang J B, Thomsen E C, Cai Q, Scarfino B J, Nie Z, Coffey G W, James W J, Yelon W B, Anderson H U and Pederson L R 2006 *J. Electrochem. Soc.* **153** J133
[11] de Lima O F, Coaquira J A H, de Almeida R L and Malik S K 2010 *J. Appl. Phys.* **107** 09E107
[12] Zhou X D, Pederson L R, Cai Q, Yang J and Scarfino B J 2006 *J. Appl. Phys.* **99** 08M918
[13] De Kalyanashis, Ray Ruma, Panda Rabi Narayan, Giri Saurav, Nakamura Hiroyuki and Kohara Takao 2005 *J. Magn. Magn. Mater.* **288** 339
[14] De K, Thakur A, Manna A and Giri S 2006 *J. Appl. Phys.* **99** 013908
[15] De K, Patra M, Majumdar S and Giri S 2008 *J. Phys. D: Appl. Phys.* **41** 175007
[16] Wu X S and Gao J 1999 *Physica C* **315** 215
[17] Wu X S, Jiang S S, Liu J, Chen W M and Jin X 1998 *Physica C* **309** 25
[18] Larson A C and Von Dreele R B 1985 *Los Alamos National Laboratory Report LAUR* **86** 748
[19] Wu X S and Gao J 1999 *Physica C* **313** 49
[20] Xie Q Y, Wu Z P, Wu X S and Tan W S 2009 *J. Alloys Compd.* **474** 81
[21] Karmakar A, Majumdar S and Giri S 2009 *Phys. Rev. B* **79** 094406
[22] Liu X J, Lia Z Q, Yu A, Liu M L, Li W R, Li B L, Wu P, Bai H L and Jiang E Y 2007 *J. Magn. Magn. Mater.* **313** 354
[23] NataliSora Isabella, Caronna Tullio, Fontana Francesca, Fernandez Cesar deJulian, Caneschi Andrea and Green Mark 2012 *J. Solid State Chem.* **191** 33
[24] Bhame S D, Joly V L Joseph and Joy P A 2005 *Phys. Rev. B* **72** 054426
[25] Thakur M, Patra M, Majumdar S and Giri S 2008 *J. Phys.: Condens. Matter* **20** 195215
[26] Tong W, Zhang B, Tan S and Zhang Y H 2004 *Phys. Rev. B* **70** 014422
[27] Hearne G R, Pasternak M P, Taylor R D and Lacorre P 1995 *Phys. Rev. B* **51** 11495
[28] Shein I R, Shein K I, Kozhevnikov V L and Ivanovskii A L 2005 *Phys. Solid State* **47** 2082